A switching scheme for synthesizing attractors of dissipative chaotic systems

Marius-F. Danca[1], Wallace K. S. Tang[2] and Guanrong Chen[2]
[1]Department of Applied Sciences, Avram Iancu University, Cluj-Napoca, Romania
[2]Department of Electronic Engineering, City University of Hong Kong, P.R. China

March 16, 2013

Abstract

In this paper, a periodic parameter-switching scheme is proposed for synthesizing a large class of hyperbolic attractors of continuous-time and autonomous dissipative chaotic systems depending linearly on a single real bifurcation parameter. It is illustrated by numerical simulations that a wide range of hyperbolic attractors can be obtained by this new scheme. The scheme can also be considered as an effective way for control and anticontrol of chaos.

keywords: attractors synthesis, chaos control, anticontrol, local attractors, global attractors

1 Introduction

A large class of chaotic systems can be represented by a continuous-time autonomous dissipative model depending linearly on a single real bifurcation parameter, expressed in the general form of the following Initial Value Problem:

$$S: \ \dot{\mathbf{x}} = f_p(\mathbf{x}), \quad \mathbf{x}(0) = \mathbf{x}_0, \tag{1}$$

where f_p is an $\mathbb{R}^n$-valued function of variable $\mathbf{x} = (x_1, x_2, \ldots, x_n)^T \in \mathbb{R}^n$, with a bifurcation parameter $p \in \mathbb{R}$ and $n \geq 3$, and has the expression

$$f_p(\mathbf{x}) = g(\mathbf{x}) + pA\mathbf{x} \tag{2}$$

in which $g : \mathbb{R}^n \longrightarrow \mathbb{R}^n$ is a continuous-time nonlinear function, A is a real constant $n \times n$ matrix, $\mathbf{x}_0 \in \mathbb{R}^n$, and $t \in I = [0, \infty)$.

Throughout, the existence and uniqueness of solutions are assumed, and it is supposed that there exist only hyperbolic equilibria.

Based on the bifurcation parameter p, different attractors can exist. However, from a practical design point of view, it is sometimes difficult to generate a specific attractor by a particular parametric value of p on a physical device. Hence, it is the objective of this paper to propose a simple scheme to implement p so that some desirable attractors can be synthesized.

The scheme is to use a time-varying, or more preciously, periodically switching parameter according to some design rules. It will be demonstrated, empirically by various experiments, that a desired attractor can be duly obtained by the proposed switching scheme. Similarly to other control methods suggested in

[1], [7], [20], this switching scheme can also be considered as a kind of chaos controller or anti-controller for a given system.

The organization of the paper is as follows. In the next section, the proposed parameter-switching scheme for synthesizing attractors is described, along with two conjectures which are fully supported by intensive simulations as further explained in Sect. 3. Finally, in Sect. 4, some concluding remarks are given and major issues for future work are discussed.

2 Synthesis of Attractors

Notation 1 *Consider the Initial Value Problem (1). Let $\mathcal{A}$ be the set of all global attractors depending on parameter p, including attractive stable fixed points, limit cycles and chaotic (possibly strange) attractors. Let also $\mathcal{P} \subset \mathbb{R}$ be the set of the corresponding admissible values of p.*

Due to the assumed dissipativity, $\mathcal{A}$ is non-empty (see e.g. [17]). It then follows naturally that for the considered class of systems, a bijection may be defined between the sets $\mathcal{P}$ and $\mathcal{A}$, although $\mathcal{A}$ is somewhat restrictive. Thus, giving any $p \in \mathcal{P}$, a unique global attractor is specified, and vice versa.

Remark 2 *The bijection between $\mathcal{P}$ and $\mathcal{A}$ is somehow connected with the known paradigm in the dynamical systems of complex variables. It is said that the Mandelbrot set is a sort of book with infinitely many pages, where each page is a picture of a Julia set corresponding to a value of the parameter identifying a point of the Mandelbrot set [19].*

In this paper, computer simulations are used as the major analytical tool. Hence, the *ω-limit set* (actually, its approximation) of the resultant trajectory is considered (see Appendix) which, as usual [9], is considered after neglecting a sufficiently long period of transients.

In order to have a measure for the "success" on attractor synthesis, it is essential to compare the numerically obtained attractors. However, the size and the shape of an attractor usually change with the control parameter, particularly when a nonlinear system is studied. Moreover, its geometric structure can be very complicated. Therefore, it is extremely difficult, if not impossible, to determine the position of a chaotic attractor in the phase space. That also appears to be true even for an equilibrium point or a periodic trajectory in general.

Recognizing the difficulties in comparing attractors, a practical (nonstandard but useful) criterion is introduced in the following:

Criterion 3 *Two attractors are considered to be* identical *if*
i) their geometrical forms in the phase space (almost) coincide;
ii) the sense of the motion is preserved.

Criterion 3 is a suitable modification and adaptation of the known concept of topological equivalence (see e.g. [12]), for practical use rather than for theoretical rigor.

This geometrical identity concept considered in $\mathbb{R}^n$, based on both phase-space and time-series representations, serves well for computer graphic inspection of attractive fixed points and limit cycles. However, the situation becomes complicated for chaotic attractors (see e.g. [8]). In this case, the almost identity of two chaotic attractors is justified by a geometric coincidence of their *branched manifolds*, known as *knot holders* (see Appendix and [22]) near the preserved sense of motion on the trajectories. In addition, phase portraits, histograms and Poincaré sections are all used as supplements for the verification of the identity of two chaotic attractors.

Remark 4 *Using Criterion 3, the invariance of branched manifolds under the changes of control-parameter values is avoided (in fact, this entire work relies on the variance on the parameter), and thus, the injectivity between $\mathcal{P}$ and $\mathcal{A}$ is not violated. Also, the use of some inherent tools of topological characterization*[1] *or dimensions related to the comparison of attractors (see, e.g., [5], [8], [12], [16], [17]) can be avoided.*

Notation 5 *Let $\mathcal{P}_N = \{p_1, p_2, \dots, p_N\} \subset \mathcal{P}$ be a finite ordered subset of $\mathcal{P}$ containing N different values of p, which determines the set of attractors $\mathcal{A}_N = \{A_{p_1}, A_{p_2}, \dots, A_{p_N}\} \subset \mathcal{A}$.*

Considering the systems modeled by (1), the following conjecture (the first main result of this paper) can be stated:

Conjecture 1. *For any finite set $\mathcal{A}_N$ of $N(\geq 2)$ attractors, corresponding to $\mathcal{P}_N$ there exists an attractor A^* generated by (1) with switching parameter p in $\mathcal{P}_N$ depending upon certain rules. Moreover, $A^* \in \mathcal{A}$, i.e. A^* is an attractor corresponding to a specific value p, which can be precisely determined.*

Remark 6 *The above conjecture seems to have its reverse form: Any attractor $A_p \in \mathcal{A}$ may be synthesized from a finite set of attractors of $\mathcal{A}$.*

Next, consider a partition of I, $I = \cup_{i\in\mathbb{N}^*}[t_{i-1}, t_i)$, with $t_0 = 0$, such that $t_i = jh$, for $i, j \in \mathbb{N}$, where h is a positive real number which will be selected empirically, and let p be determined by a piecewise continuous function $\psi : I \longrightarrow \mathcal{P}_N$, defined by

$$\psi(t) = p_k \text{ for } t \in [t_{i-1}, t_i), \quad i \in \mathbb{N}^*, \ k \in \{1, 2, \dots, N\}, \ p_k \in \mathcal{P}_N. \tag{3}$$

Thus, a trajectory of system (1) can be partitioned, as depicted for a particular case in Fig. 1 (a), based on the switching scheme described in Fig. 1 (b). In all of our simulations, the system trajectories are numerically obtained based on a fixed step-size integration with the integration step-size h.

The switching synthesis rule in Conjecture 1 can be defined as the following $(m_1 + m_2 + ... + m_N)h$ -periodic sequence:

$$[m_1 p_{\varphi(1)}, \ m_2 p_{\varphi(2)}, \dots, m_N p_{\varphi(N)}], \tag{4}$$

where the weights m_i are some positive integers and φ permutes the subset $\{1, 2, \dots, N\}$.

Scheme (4) has the following significance: the numerical method will integrate (1) with $p = p_{\varphi(1)}$ in the first m_1 steps, and then with $p = p_{\varphi(2)}$ in the next m_2 steps, and so on, until the last Nth subinterval. The cycle is then repeated so that a periodic parameter-switching scheme is obtained.

For example, the sequence $[7p_2, 3p_1, 4p_3]$ (see Fig. 1 (b)) implies that, for the first 7 integration steps, $p = p_2$, and then for the next 3 integration steps, $p = p_1$, and for the last 4 steps, $p = p_3$. After that, the cycle is repeated again, i.e., $[7p_2, 3p_1, 4p_3]$ should be understood as being the following periodical sequence:

$$7p_2, 3p_1, 4p_3, 7p_2, 3p_1, 4p_3, 7p_2, 3p_1, 4p_3, \dots.$$

As justified with the averaging system and demonstrated by the simulation results, Conjecture 1 is reformulated in the following more practical form, so that parameter p can be estimated.

Conjecture 2. *For any finite set of attractors $A_N \in \mathcal{A}$, there exists a set of N positive integers, $m_i, i = 1, 2, \cdots, N$, such that, based on the integration scheme (4), a synthesized attractor A^* can be*

[1] For example, considering the shape of an attractor, it is possible to have two attractors possessing the same shape and however being different in the sense of Criterion 3.

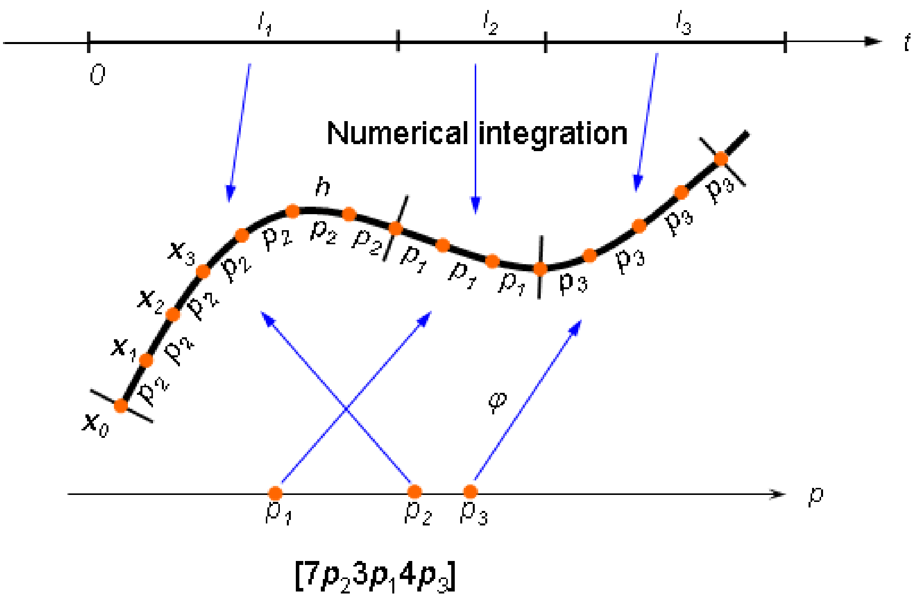

(a)

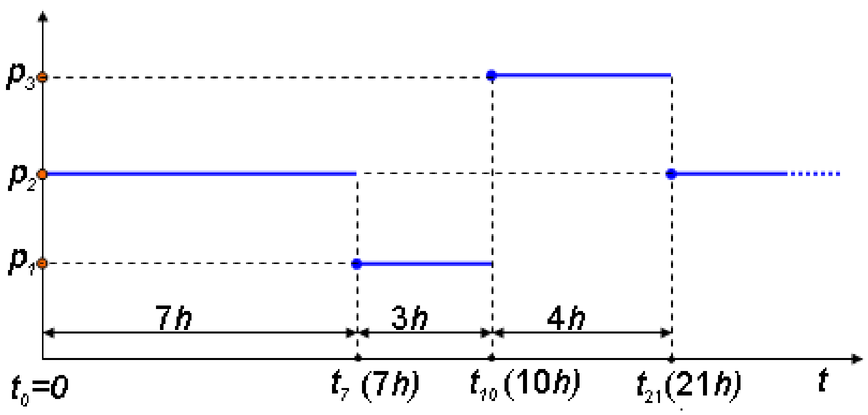

(b)

Figure 1: Sketch of the scheme (3), (4), partition interval for $N = 3$ for the case $[7p_2, 3p_1, 4p_3]$; $m_1 = 7$, $m_2 = 3$ and $m_3 = 4$. a) trajectory partition; b) parameter variance vs time.

obtained, which is identical (in the sense of Criterion 3) to an attractor $A_p \in \mathcal{A}$ with p being given by the following relation:

$$p = \frac{\sum_{k=1}^{N} p_{\varphi(k)} m_k}{\sum_{k=1}^{N} m_k}. \tag{5}$$

For example, referring to the bifurcation diagram of Chen's system, given in Fig. 2, it is possible to obtain a chaotic attractor A^* identical to A_p, with $p = 24.532$ based on the switching sequence, $[1p_1, 1p_2]$ with $p_1 = 23.014$ and $p_2 = 26.08$, following (5) ($p = (p_1 + p_2)/2 = 24.532$). Similarly, one can have a synthesized periodic attractor identical to A_p, with $p = 26.083$ if $[2p_1, 1p_2]$ is used with $p_1 = 25.75$ and $p_2 = 26.25$.

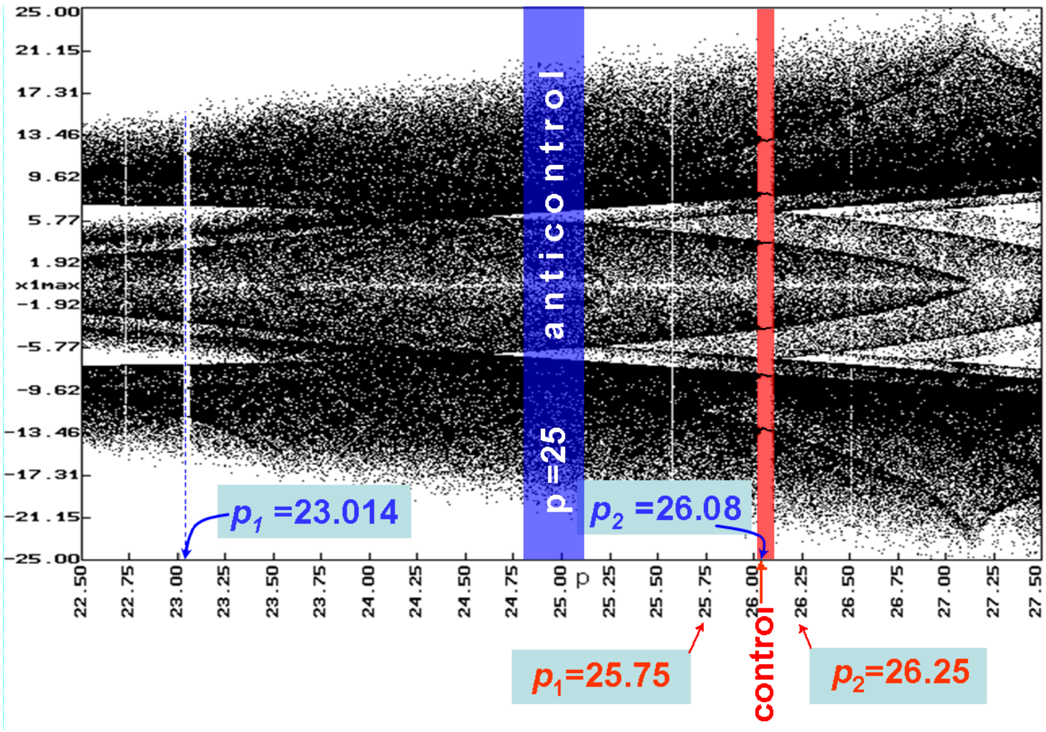

Figure 2: Bifurcation diagram of x_1 with $\mathcal{P} = [22.50,\ 27.50]$ for Chen's system.

Remark 7

1. *There is only one pseudo-identity in synthesizing chaotic attractors if p given in (5) is an irrational number due to numerical errors (see Table 4). In this case, small difference can appear in between the two attractors, A^* and A_p.*

2. *Because of the resemblance of the relation (5) to a weighted average formula, one may consider the synthesized attractor A^* as an* averaged attractor, *the value p as an* averaged value, *and m_k as weights.*

3. *Equation (5) represents an affine combination because one may write $p = \sum_{k=1}^{N} \alpha_k p_{\varphi(k)}$ with $\alpha_k = m_k \Big/ \sum_{k=1}^{N} m_k$, such that $\sum_{k=1}^{N} \alpha_k = 1$. Therefore, by the nature of this algorithm, $\mathcal{A}$ may be viewed as a* vector space *and $\mathcal{P}$ as a* field, *so any element (vector) of $\mathcal{A}$ could be considered as being synthesized from a set of a finite number of vectors in $\mathcal{A}$, with coefficients in $\mathcal{P}$.*

4. *For any ordered set $\mathcal{P}_N = \{p_{\min}, \ldots, p_{\max}\}$, using scheme (4) the resultant averaged p, given by (5), is located inside the interval $[p_{\min}, p_{\max}]$, i.e., $p_{\min} \leq p \leq p_{\max}$. Thus, if $\mathcal{P}_N$ is chosen within a chaotic (or periodic) band in the bifurcation diagram, the resultant attractor will also be chaotic (or periodic), while if $\mathcal{P}_N$ is chosen within disjoint bands the resultant attractor could be of any type. In addition, the synthesized attractor A^* has a well-defined position in the parameter space, i.e., 'inside' the set of attractors $A_{p_{\min}}, \ldots, A_{p_{\max}}$, ordered in the parameter space (bifurcation diagram) by the order induced from $\mathcal{P}$ being close to one of the attractors A_{p_k} with corresponding values of m_k. For example, if $N = 2$, and p_1 and p_2 are chosen from the bifurcation diagram, then the synthesized attractor A^* is situated in the parameter space between the attractors A_{p_1} and A_{p_2}. Thus, if $m_1 > m_2$, then A^* is closer to A_{p_1}. Consequently, a density-like property of the attractors on $\mathcal{A}$ could be observed: between any two arbitrarily close attractors, there always exists another attractor.*

5. *Following Remark 7.4 above, even if the switch of p is relatively large, A^* will remain inside the range $A_{p_{\min}}, \ldots, A_{p_{\max}}$. However, for critical values of m (see Remark 3 below) the identity between A^* and A_p may be compromised.*

6. *Generally, for a fixed initial condition $\mathbf{x}_0$, (5) is not 'commutative', i.e. $[m_1p_1, m_2p_2]$ and $[m_2p_2, m_1p_1]$ generally give different attractors.*

3 Numerical Results and Applications

In this section, it is to demonstrate the synthesis of a particular attractor based on the switching scheme described in the last section. The scheme has been applied to three different chaotic systems, namely the Chen's system, the Lorenz system and the Rössler system.

The dynamical equations of these three systems are first recalled, as follows:

Chen's System: [4]

$$\begin{aligned} \dot{x}_1 &= a(x_2 - x_1), \\ \dot{x}_2 &= (p - a)x_1 - x_1x_3 + px_2, \\ \dot{x}_3 &= x_1x_2 - bx_3, \end{aligned} \tag{6}$$

with parameters $a = 35$ and $b = 3$, while p is chosen as the control parameter here.

Referring to (2), one has

$$g(\mathbf{x}) = \begin{pmatrix} a(x_2 - x_1) \\ -x_1x_3 - x_2 \\ x_1x_2 - cx_3 \end{pmatrix}, \quad A = \begin{pmatrix} 0 & 0 & 0 \\ 1 & 0 & 0 \\ 0 & 0 & 0 \end{pmatrix}.$$

Lorenz System:

$$\begin{aligned} \dot{x}_1 &= a(x_2 - x_1), \\ \dot{x}_2 &= x_1(p - x_3) - x_2, \\ \dot{x}_3 &= x_1x_2 - cx_3, \end{aligned} \tag{7}$$

with $a = 10$ and $c = 8/3$, and p again is the control parameter. Here,

$$g(\mathbf{x}) = \begin{pmatrix} a(x_2 - x_1) \\ -x_1x_3 - x_2 \\ x_1x_2 - cx_3 \end{pmatrix}, \quad A = \begin{pmatrix} 0 & 0 & 0 \\ 1 & 0 & 0 \\ 0 & 0 & 0 \end{pmatrix}.$$

Rössler System:

$$\begin{aligned} \dot{x}_1 &= -x_2 - x_3, \\ \dot{x}_2 &= x_1 + ax_2, \\ \dot{x}_3 &= b + x_3(x_1 - p), \end{aligned} \tag{8}$$

with $a = b = 0.1$, and p is the control parameter and

$$g(\mathbf{x}) = \begin{pmatrix} -x_2 - x_3 \\ x_1 + ax_2 \\ b + x_3x_1 \end{pmatrix}, \quad A = \begin{pmatrix} 0 & 0 & 0 \\ 0 & 0 & 0 \\ 0 & 0 & -1 \end{pmatrix}.$$

Based on the parameter-switching scheme (4), it is possible to synthesize any attractor of the considered systems. Here, the switching scheme $[m_1p_2, m_2p_1, m_3p_3]$ is applied to the three different systems while the simulation settings and results are summariized in Table 1.

System	Switching scheme	p_1	p_2	p_3	Averaged value p	A^*	Graphical results
Chen	$[7p_2, 3p_1, 4p_3]$	23.014	24	32.0195	26.080	*periodic*	Fig. 3
Lorenz	$[8p_2, 7p_1, 2p_3]$	10	125.5	130	78.4706	*chaotic*	Fig. 4
Rössler	$[2p_2, 5p_1, 3p_3]$	18	25	31	23.300	*chaotic*	Fig. 5

Table 1: Testing cases for synthesizing attractors with scheme $[m_1p_2, m_2p_1, m_3p_3]$. The simulation time T was set to 75 and the integration step size $h = 0.001$.

The simulation time T is chosen empirically, so that it was large enough to confidently verify the results but the presented images have relatively small T in order to obtain clear pictures. Also, in most cases, the transients were neglected. In addition, special attention is paid to $\mathbf{x}_0$ in order to focus on the same attractor.

The averaged value p is computed by (5), for example, considering the Chen attractor, $p = (7 \times p_2 + 3 \times p_1 + 4 \times p_3)/(7 + 3 + 4) = 26.080$.

In order to justify the identity of the obtained attractors, the phase portraits and the histograms are both provided. For the case of having a synthesized chaotic attractor, the Poincaré sections are also obtained for comparison. As reflected by the simulation figures, the synthesized attractors are more or less identical to the one given by the averaged value. Some additional remarks are given as follows:

Remark 8

1. *Better synthesis results are observed in Chen and Lorenz systems, while small derivation is noticed in the case of the Rössler system. It may be due to the sensitivity of the computed results to the integration time-steps in the Rössler system as pointed out in [21].*

2. *Because of the stiffness or strong dependence on the integration step size in some cases, some trajectories of A^* present 'corners' especially near the peaks, where the performances of any numerical method are fully stressed. In our tests, the Rössler system presents this phenomenon (see Fig. 5 (b)). However, even in this case, the two attractors A^* and A_p are well matched.*

   The solution would be more accurate if smaller step size, or adaptive step size or multistep numerical methods, are used. It should also be noticed that a special numerical method [6] is utilized for the Chen system due to its stiffness.

3. *Let $m_k = \max\{m_1, \ldots, m_N\}$. If m_k has a relatively large value (10 in our experiments) then A^* still remains in a relatively small neighborhood of A_p but it presents some oscillations (for example, the result with $[7p_2, 3p_1, 10p_3]$ is depicted in Fig. 6). If this value exceeds 50, say, then A^* moves closer to the attractor corresponding to p_k and a larger deviation in the resultant attractor is expected.*

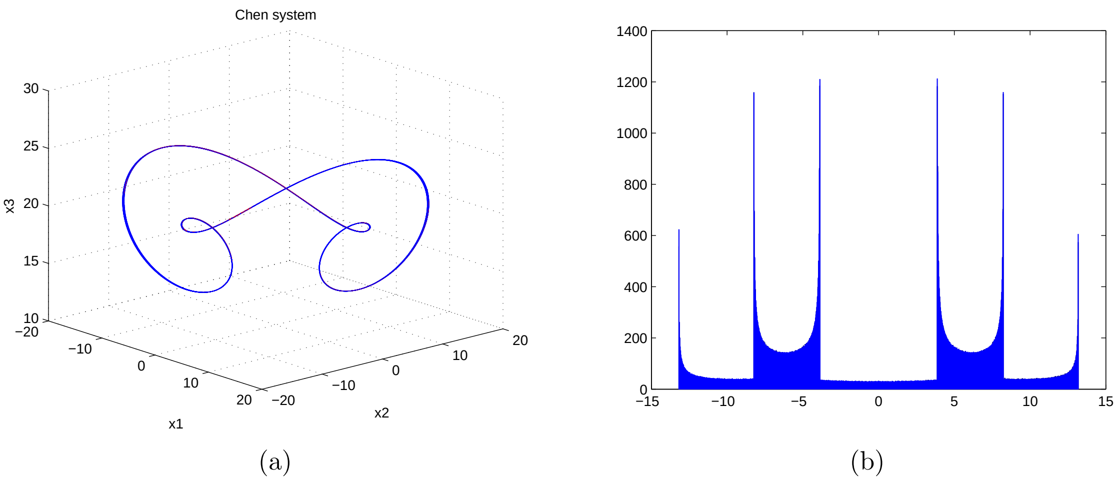

Figure 3: Synthesized limit cycle A^* from the Chen system, with $[7p_2, 3p_1, 4p_3]$, $p_1 = 23.014$, $p_2 = 24$, $p_3 = 32.0195$, $T = 75$ and $h = 0.001$. a) Phase portraits of A^* and A_p ($p = 26.080$), superimposed; b) Histogram of A^* and A_p, superimposed.

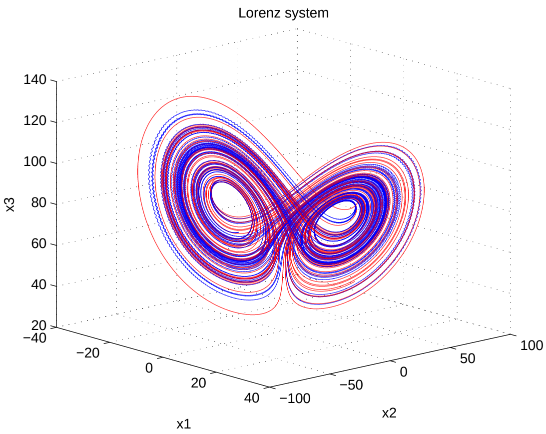

(a)

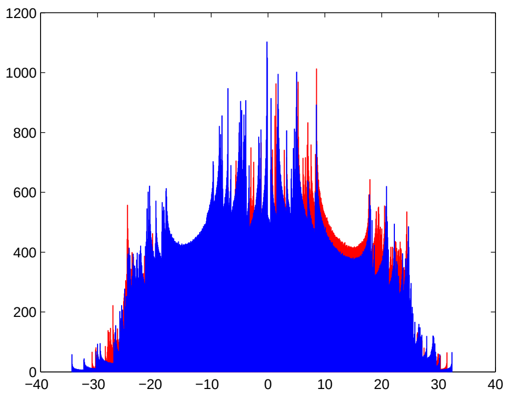

(b)

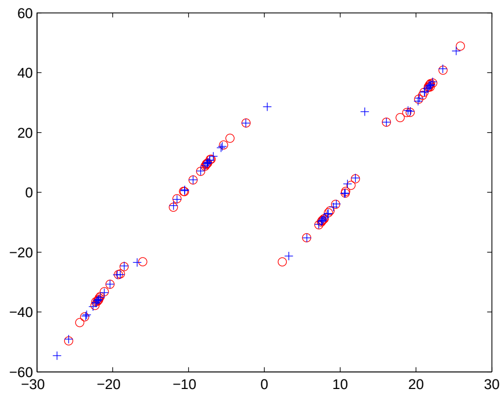

(c)

Figure 4: Synthesized the chaotic Lorenz attractor A^*, with $[8p_2, 7p_1, 2p_3]$, $p_1 = 103$, $p_2 = 125.5$, $p_3 = 130$, $T = 75$ and $h = 0.001$. a) Phase portrait of A^* and A_p ($p = 78.4706$), superimposed; b) Histogram of A^* and A_p, superimposed; c) Poincaré section of A^* and A_p, superimposed.

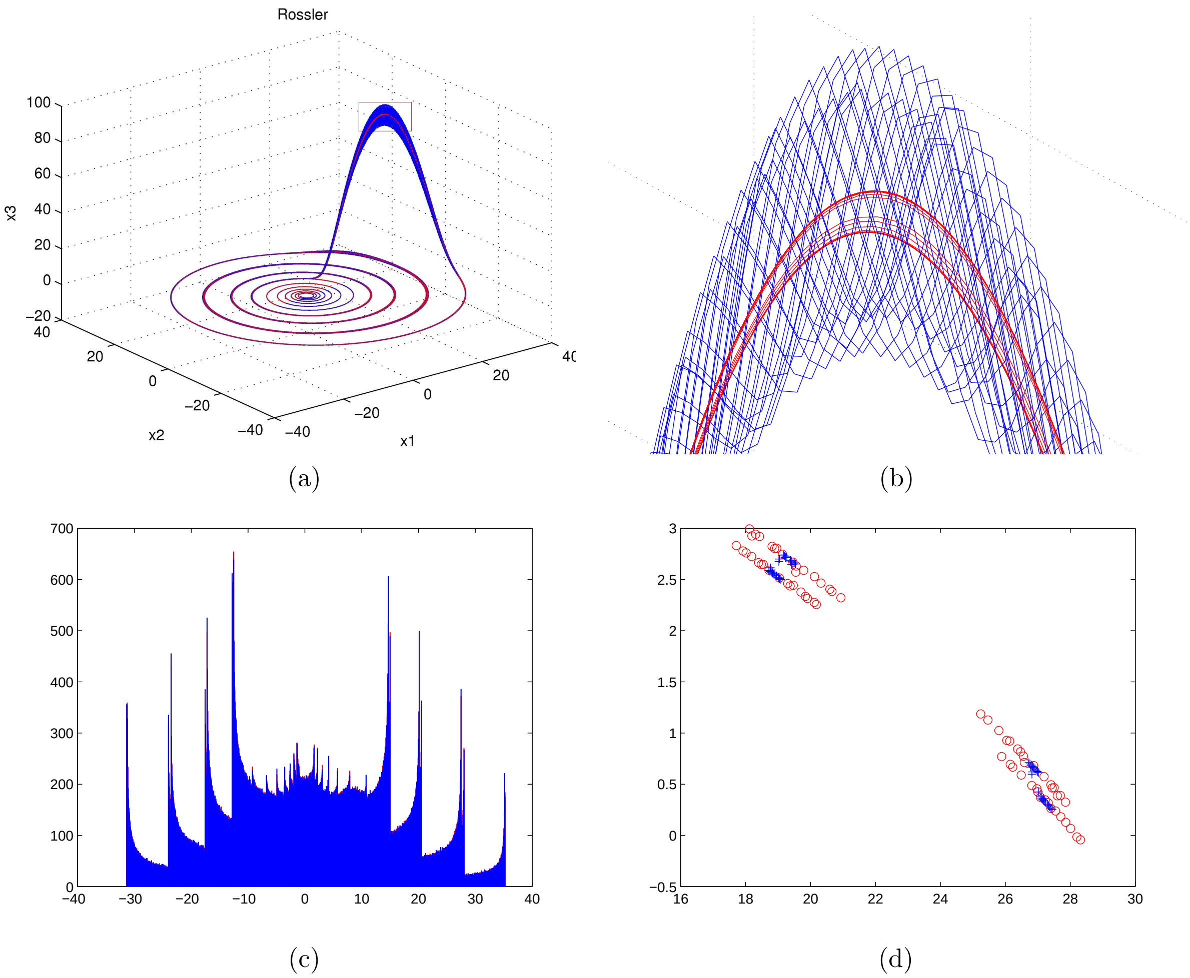

Figure 5: Synthesized limit cycle A^* from the Rössler system, with $[2p_2, 5p_1, 3p_3]$, $p_1 = 18$, $p_2 = 25$, $p_3 = 31$, $T = 75$ and $h = 0.001$. a) Phase portrait of A^* and A_p ($p = 23.3$), superimposed; b) A zoom-in window of the phase portrait c) Poincaré section of A^* and A_p, superimposed; d) Histogram of A^* and A_p, superimposed.

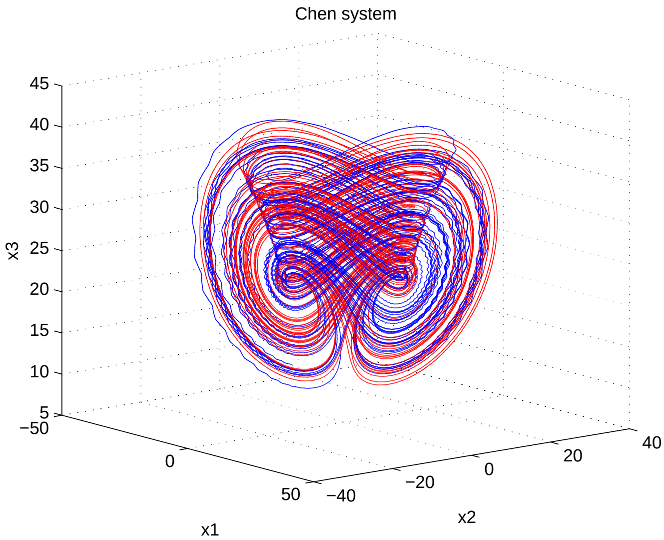

Figure 6: Phase portrait of A^* and A_p synthesized from the Chen system with $[7p_2, 3p_1, 10p_3]$, $p_1 = 23.014$, $p_2 = 24$, $p_3 = 32.0195$, $T = 75$ and $h = 0.001$.

3.1 Control and Anticontrol of Chaos

The proposed scheme can be adopted as an approach for chaos anticontrol and control. For practical reasons, we consider $N = 2$, i.e. the switch is only between two parameter values: p_1 and p_2. In this case, the possible situations which could arise are presented in Table 2.

chaos+chaos=chaos

chaos/order+order/chaos=chaos/order

order+order=order

order+order=chaos (anticontrol)[2]

chaos+chaos=order (control)

Table 2. The possible combinations between order and chaos

Because of the empirical character of the switch method, its utilization is more theoretical than practical. However, the switching scheme gives some new interpretations to the control and anticontrol of chaos.

[2]This kind of anticontrol situation is a variant of Parrondo's paradox [13], which states the following strategy: losing+losing=winning, i.e., chaos+chaos=order (see [1] and [20], where variants in the discrete case are presented).

3.2 Anticontrol of Chaos

Consider a dynamical system modeled by (1)–(2), with p_1 and p_2 corresponding to regular motions (i.e., A_{p_1} and A_{p_2} are attracting fixed points and/or stable limit cycles). Applying scheme (4) with adequate (empirically chosen) m_1, m_2, and h, a chaotic attractor A^* may be synthesized, where the corresponding value p of A_p is given by (5), as confirmed by the following experiments.

For comparison, in all the presented results below, the time series of A^* (the corresponding system being denoted by S) and his phase portraits are drawn in blue, while the phase portraits corresponding to A_p are drawn in red. The systems corresponding to p_1 and p_2 are denoted by S_1 and S_2, and their time series being depicted with red and green curves, respectively.

3.2.1 Chen System

To better understand the way in which scheme (4) behaves, the bifurcation diagram of state variable x_1 given in Fig. 2 is referred.

According to the affine property mentioned in Remark 7.4, it is possible to synthesize an attractor in between two single intervals from which p_1 and p_2 are chosen. For example, let $p_1 = 23.014$ and $p_2 = 26.05$ correspond to two periodic attractors (Fig. 2), with their time series being depicted in Fig. 7 (a). The relatively large blue band in the bifurcation diagram (Fig. 2) indicates that one may obtain the expected chaotic attractors corresponding to a relatively large p-interval, between p_1 and p_2.

Now, letting $m_1 = 1$ and $m_2 = 1$, and using scheme $[1p_1, 1p_2]$, a chaotic attractor is indeed obtained. By (5), one has $p = (p_1 + p_2)/2 = 24.532$ which, taking into account also the bifurcation diagram, signifies a chaotic attractor. Taking integration step size $h = 0.001$ with $T = 75$, the time series, phase portrait and Poincaré section of the synthesized results, are shown in Fig. 7 (a)–(c), respectively.

For comparison, the phase portrait and Poincaré section of the attractor A_p are also drawn in Fig. 7 (b) and (c), respectively. It can be clearly observed that the two attractors A^* and A_p are identical in the sense of Criterion 3.

3.2.2 Lorenz System

Selecting $p_1 = 93$ and $p_2 = 100$, which correspond to two different periodic attractors (as drawn in red and in green respectively in Fig. 8 (a)), a chaotic attractor can be duly obtained by using scheme $[1p_1, 1p_2]$, with $h = 0.001$ and $T = 75$, as shown in Fig. 8 (a). Similarly, the synthesized attractor is identical to the one with p given by (5), $p = 96.5$, as shown in Figs. 8 (b) and (c).

3.2.3 Rössler System

The switching scheme is chosen with $p_1 = 6$, $p_2 = 12.5$, $m_1 = m_2 = 1$ and $[1p_1, 1p_2]$, and applied to the Rössler System. The integration step is modified to be $h = 0.002$, and the final simulation time is $T = 200$. Due to the sensitivity of the computed results to the integration time-steps in the Rössler system [21], some small differences between attractors A^* and A_p can be seen in Fig. 9. However, it can still be concluded that the synthesized chaotic attractor is well matched by the one generated by (5) with $p = 9.25$.

The results are depicted in Table 3.

System	Switching Sequence	p_1	p_2	Averaged value (p)	Simulation time (T)	Integration step (h)	Graphical results
Chen	$[1p_1, 1p_2]$	23.014	26.05	24.532	75	0.001	Fig. 7
Lorenz	$[1p_1, 1p_2]$	93	100	96.5	100	0.001	Fig. 8
Rössler	$[1p_1, 1p_2]$	6	12.5	9.25	200	0.002	Fig. 9

Table 3. Anticontrol of chaos using the switching scheme $[p_1, p_2]$.

3.3 Control of Chaos

Based on the same concept of synthesis, two values of p_1 and p_2, both corresponding to chaotic behaviors, with a particular choice of m_1, m_2 and h, are considered. The synthesized attractors could present regular motions. The three typical chaotic systems studied above are once again considered here.

3.3.1 Chen System

Based on (6), for $p_1 = 25.75$ or $p_2 = 26.25$, from the bifurcation diagram in Fig. 2, chaotic attractors are obtained. Assuming $m_1 = 2$ and $m_2 = 1$ and using the switching scheme $[2p_2, 1p_1]$ with integration step $h = 0.01$ and $T = 75$, the chaotic attractor corresponding to $p = (2 \times 26.25 + 25.75)/3 = 26.083$ is duly synthesized, as shown in Fig. 10.

3.3.2 Lorenz System

The result for the Lorenz system is depicted in Fig. 11. Choosing $p_1 = 90$ and $p_2 = 96$ with $m_1 = m_2 = 1$, $h = 0.001$, $T = 75$, and using the scheme $[1p_1, 1p_2]$, the resulting attractor corresponds to a stable limit cycle with the calculated value $p = 93$.

3.3.3 Rössler System

For the Rössler system, the control was achieved by applying the scheme $[1p_1, 2p_2]$ with $p_1 = 12.5$, $p_2 = 6$, $h = 0.01$ and $T = 800$. The results, with $p = 8.1(6)$, are shown in Fig. 12, which clearly confirms the statement given in Conjecture 2 (see also Remark 7.1).

The results are summarized in Table 4.

System	Switching Sequence	p_1	p_2	Averaged value (p)	Simulation time (T)	Integration step (h)	Graphical results
Chen	$[2p_2, 1p_1]$	25.75	26.25	26.083	75	0.01	Fig. 10
Lorenz	$[1p_1, 1p_2]$	90	96	93	75	0.001	Fig. 11
Rössler	$[1p_1, 2p_2]$	12.5	6	8.1(6)	800	0.01	Fig. 12

Table 4. Chaos control using the switching scheme $[m_1p_1, m_2p_2]$.

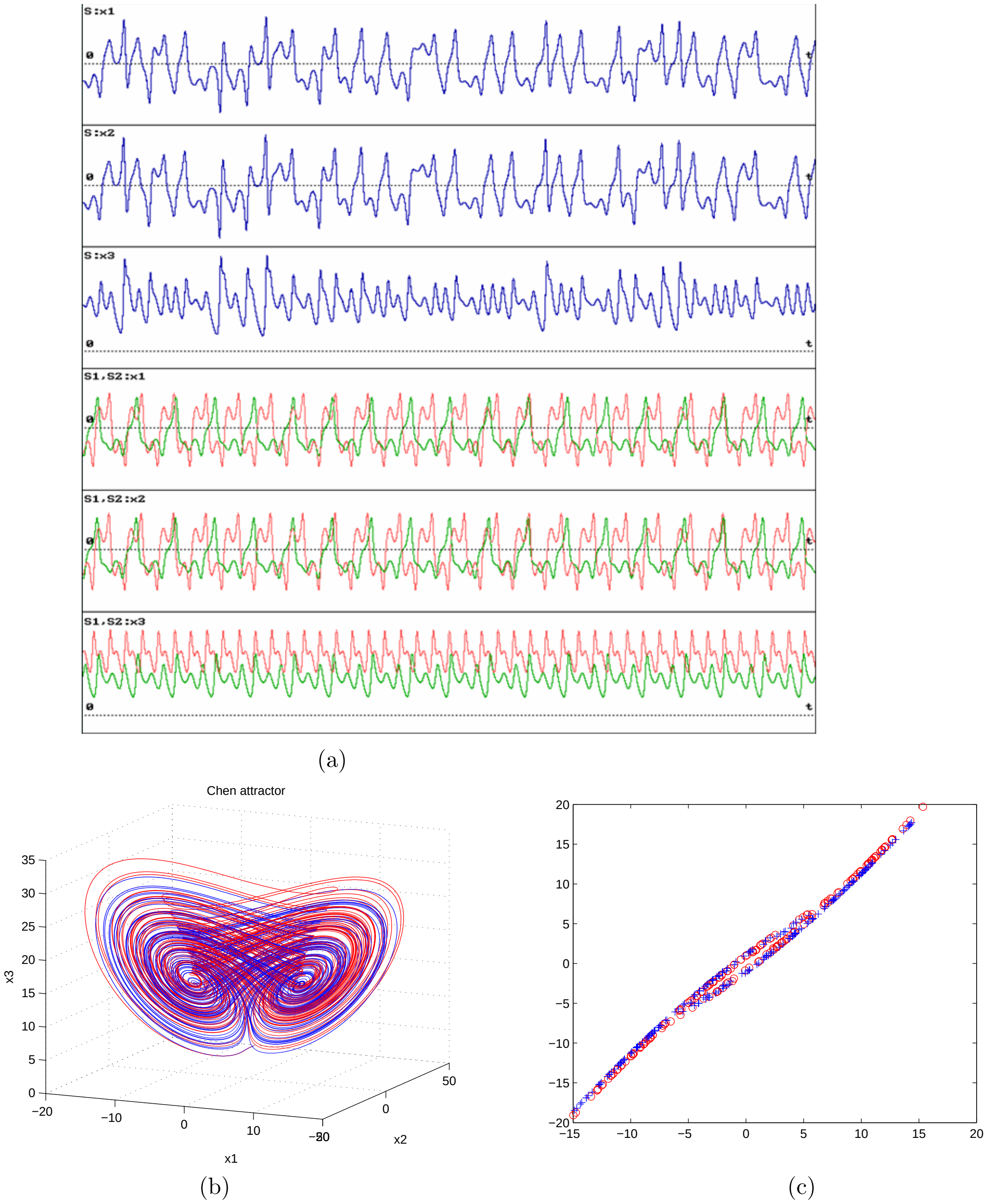

Figure 7: Synthesized the chaotic Chen attractor A^* with $[1p_1, 1p_2]$, $p_1 = 23.014$, $p_2 = 26.05$, $T = 75$ and $h = 0.001$. a) Time series; b) Phase portrait of A^* and A_p ($p = 24.532$), superimposed; c) Poincaré section of A^* and A_p, superimposed.

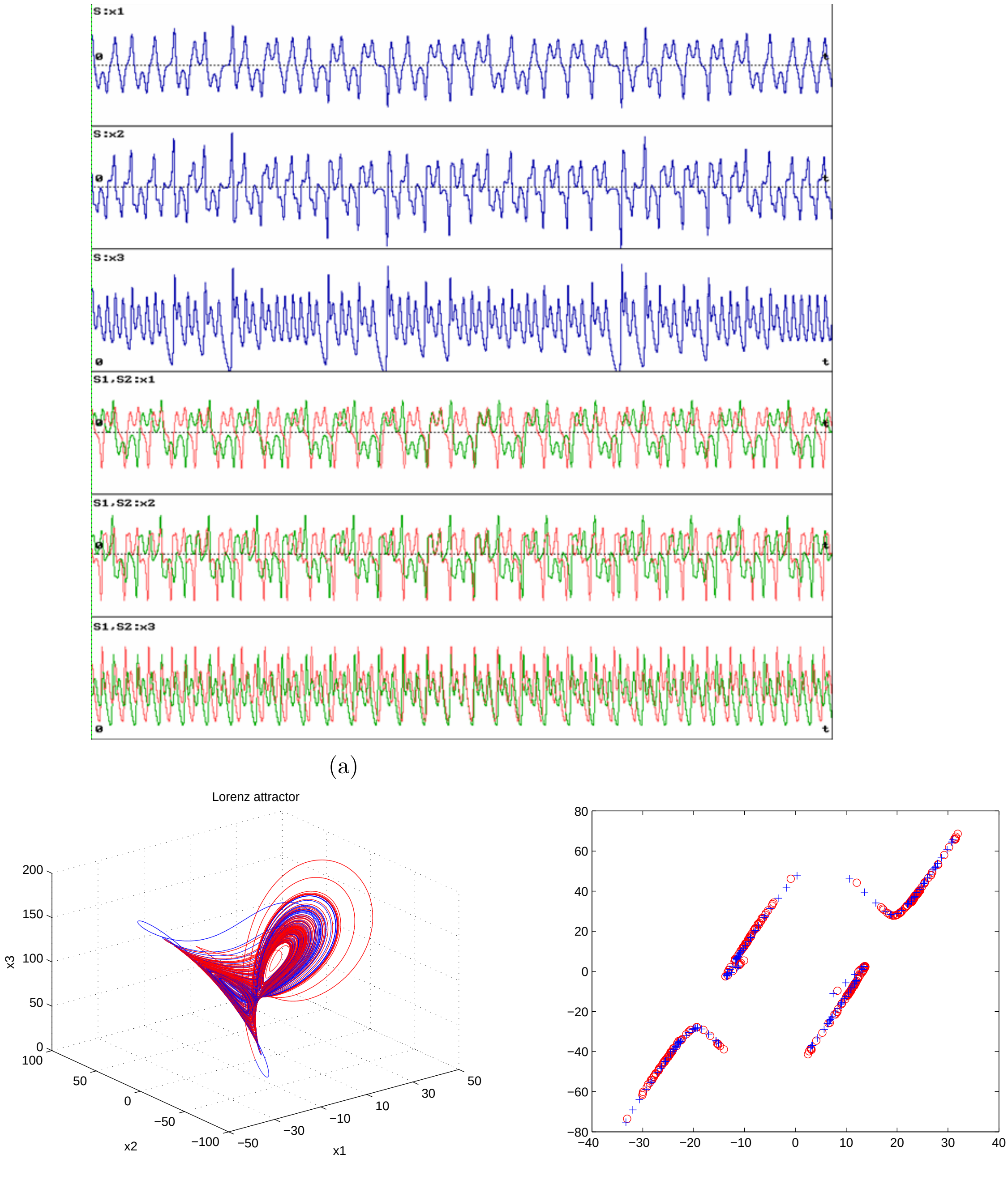

(a) (b) (c)

Figure 8: Synthesized the chaotic Lorenz attractor A^*, with $[1p_1, 1p_2]$, $p_1 = 93$, $p_2 = 100$, $T = 75$ and $h = 0.001$. a) Time series; b) Phase portrait of A^* and A_p ($p = 96.5$), superimposed; c) Poincaré section of A^* and A_p,superimposed.

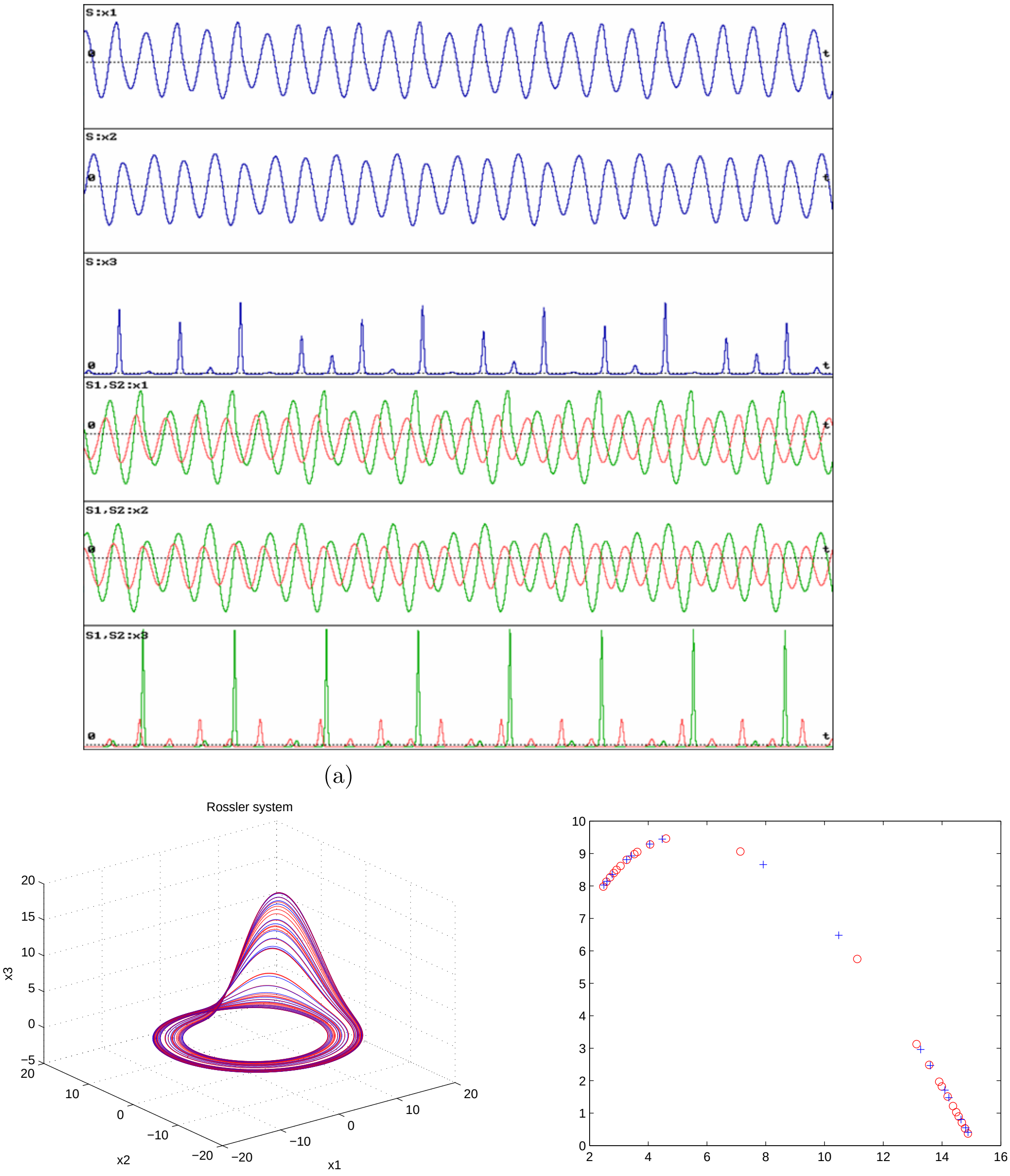

(b) (c)

Figure 9: Synthesized the chaotic Rössler attractor A^*, with $[1p_1, 1p_2]$, $p_1 = 6$, $p_2 = 12.5$, $T = 200$ and $h = 0.002$. a) Time series; b) Phase portrait of A^* and A_p ($p = 9.25$), superimposed; c) Poincaré section of A^* and A_p, superimposed.

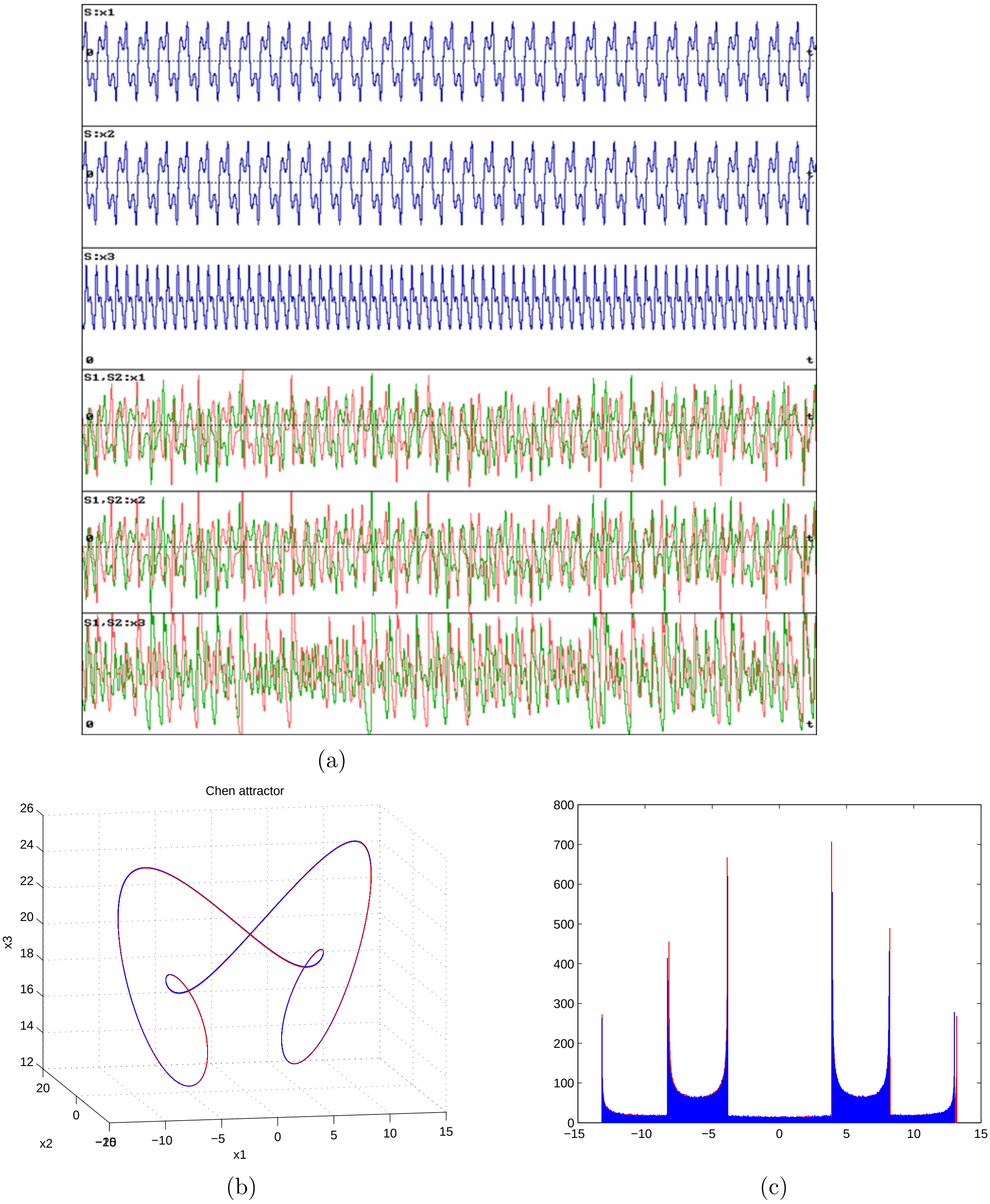

Figure 10: Synthesized limit cycle A^* from the Chen system, with $[2p_2, 1p_1]$, $p_1 = 25.75$, $p_2 = 26.25$, $T = 75$ and $h = 0.001$. a) Time series; b) Phase portrait of A^* and A_p ($p = 26.083$), superimposed; c) Histogram of A^* and A_p, superimposed.

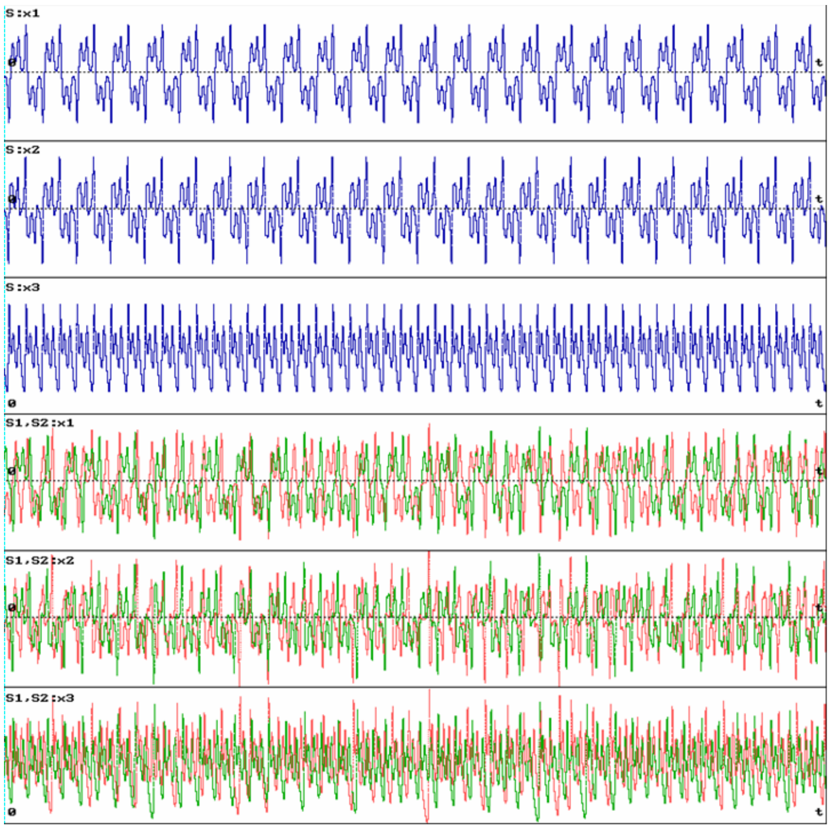

(a)

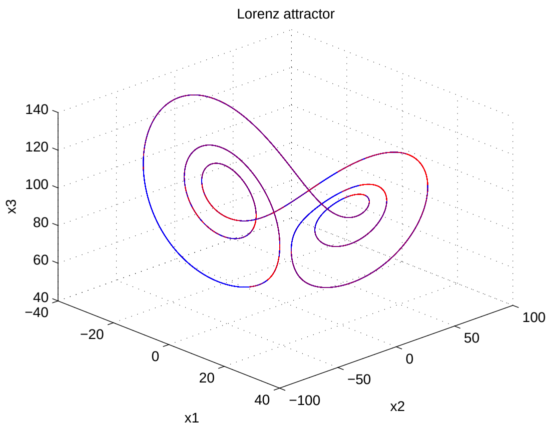

(b)

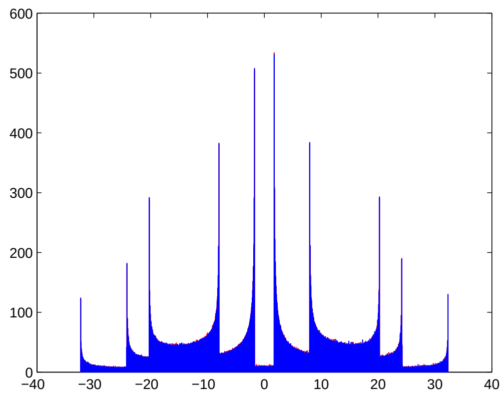

(c)

Figure 11: Synthesized limit cycle A^* from the Lorenz system, with $[1p_1, 1p_2]$, $p_1 = 90$, $p_2 = 96.25$, $T = 75$ and $h = 0.001$. a) Time series; b) Phase portrait of A^* and A_p $(p = 93)$, superimposed; c) Histogram of A^* and A_p, superimposed.

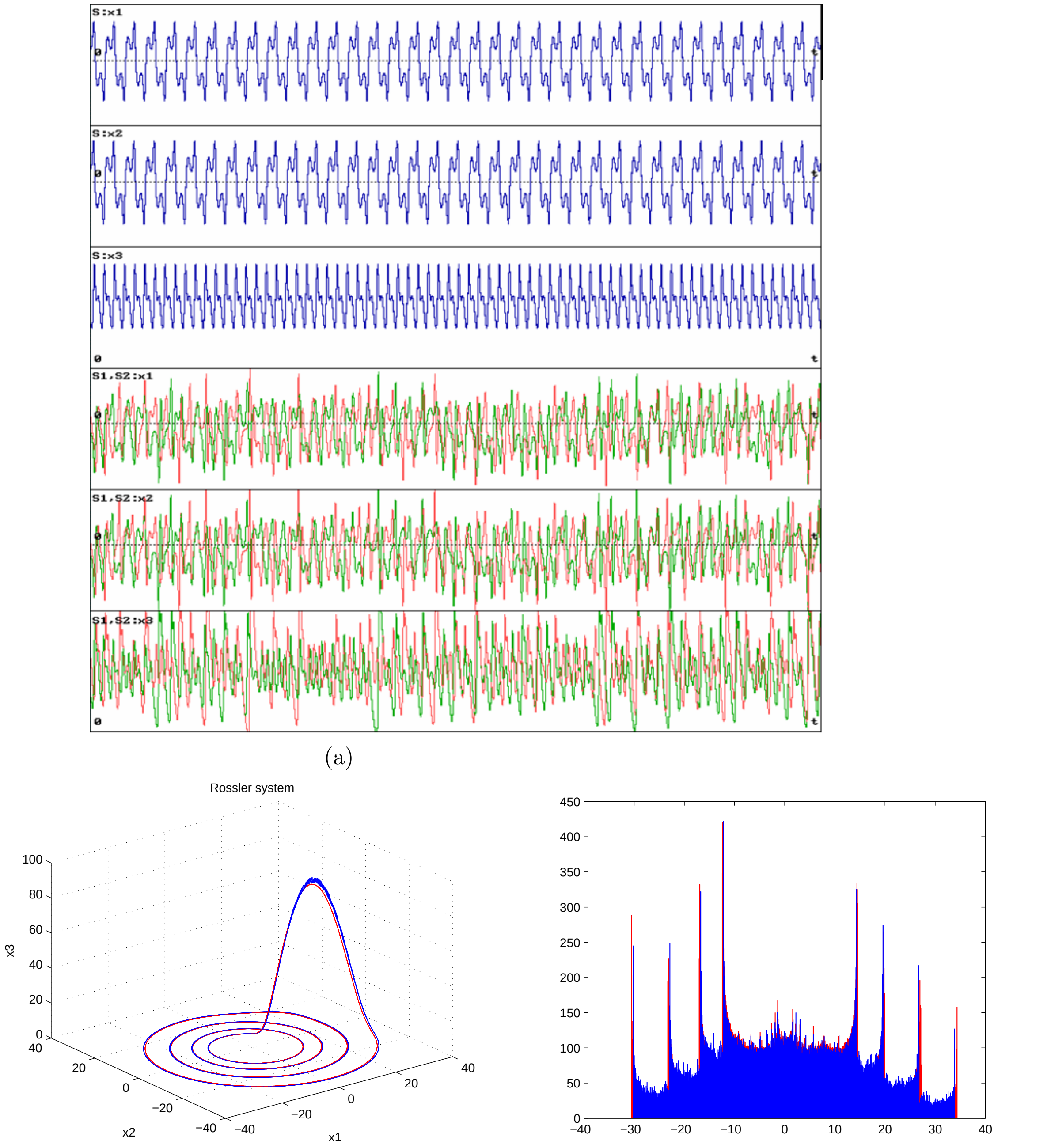

(a)

(b)

(c)

Figure 12: Synthesized limit cycle A^* from the Rössler system with $[1p_1, 2p_2]$, $p_1 = 12.5$, $p_2 = 6$, $T = 800$ and $h = 0.01$. a) Time series; b) Phase portrait of A^* and A_p ($p = 8.1(6)$), superimposed; c) Histogram of A^* and A_p, superimposed.

Remark 9

1. *The scheme is workable for chaos control (or anticontrol) only if there exists two disjointed chaotic (or periodic) windows, separated by at least one periodic (or chaotic) window.*
2. *It is possible to obtain a desired attractor $A_{\overline{p}}$, starting from two given p_1 and p_2. For this purpose, one has to solve the equation $(m_1p_1 + m_2p_2)/(m_1 + m_2) = \overline{p}$, the unknowns being m_1 and m_2.*
3. *To further elaborate, let us consider the Lorenz system (7) formulated as follows:*

$$\begin{aligned} \dot{x}_1 &= a(x_2 - x_1), \\ \dot{x}_2 &= (p_1 + u)x_1 - x_1x_3 - x_2, \\ \dot{x}_3 &= x_1x_2 - bx_3, \end{aligned} \tag{9}$$

where u is the parameter-perturbation to be injected.

For chaos control, assuming that a chaotic attractor is present with the parameter value $p = p_1$, it is possible to design a periodic pulse perturbation on parameter p_1 using u with amplitude $(p_2 - p_1)$, having m_1 off- and m_2 on-cycles. The resultant p is then governed by (5). As a result, a periodic or a fixed attractor can be obtained, as demonstrated in Fig. 11.

The same idea could be applied to anticontrol of chaos, where $p = p_1$ corresponds to a periodic or fixed-point attractor, and the control signal is again a periodic pulse with amplitude $(p_2 - p_1)$, having m_1 off- and m_2 on-cycles. The anticontrol effect is exactly equivalent to the result obtained in Fig. 8.

4 Conclusions and Discussion

In this paper, a close relationship between the system parameter and its corresponding attractor, consequently the “synthesis of attractors”, has been explored and analyzed.

For a chaotic system depending on a single real parameter, based on the conjectures given in this paper which are supported by intensive simulations, it is concluded that every attractor depending on the parameter p can be synthesized by the proposed periodic parameter switching scheme.

Moreover, this relationship suggests a symbolic interpretation of any attractor generated by the proposed scheme based on a sequence of parameters. Thus, in view of the scheme, an attractor could be described by an infinite number of periodic symbolic notations (even when the attractor is chaotic!). A relevant study, also based on symbolic sequences but for discrete maps, was recently carried out in [24].

It should be emphasized that, to our knowledge, existing analytic techniques are unable to be applied to explain the presented results. In this study, a large variety of parameters are allowed to use, and it simply violates the basic assumption of having small parameter and variations in the typical existing theoretical methods. Certainly, a rigorous proof of the proposed scheme is in order, which will be further pursued in the near future.

5 Acknowledgement

The work described in this paper was carried out when M.-F.Danca visited the Centre for Chaos and Complex Networks at the City University of Hong Kong under the support of the CityU SRG Project No. 7002134.

The authors thank Adelina Georescu and Miguel Romera for their valuable discussions and suggestions.

Appendix: Basic Concepts and Notions

Since the paper mostly deals with attractors of dynamical systems, some relevant concepts and notation, including semiflow, trajectory, global and local attractors, ω-limit set, branched manifolds, etc., are defined here for convenience. A more detailed background can be referred to the cited references, or [18].

Definition 1 *A map $\Phi : \mathbb{R}^n \times I \longrightarrow \mathbb{R}^n$ is a* semiflow *on $\mathbb{R}^n$, if*
(i) $\Phi(0, x) = x$, $x \in \mathbb{R}^n$;
(ii) $\Phi(t + s, x) = \Phi(t, \Phi(s, x))$, $t, s \in I$;
(iii) the map $(t, x) \mapsto \Phi(t, x)$is continuous.

System (1) describes a semiflow.

Definition 2 *For any $x \in \mathbb{R}^n$, the* positive trajectory *$\Gamma(x)$ through x is $\Gamma(x) = \bigcup_{t \in I} \Phi(t, x)$.*

For simplicity, the term *trajectory* has been used.

Definition 3 *A* global attractor *of S is a compact set composing of all bounded global trajectories of system (1) (see [16]).*

The study of global attractors (also known as 'global minimal B-attractor', 'global uniform attractor' or 'maximal attractor' [16]) is a major research topic in dynamical systems, in particular within the context of PDEs (see e.g. [23]). From the definition, a global attractor contains all the dynamics evolving from all possible initial conditions. In other words, it contains all solutions, including stationary solutions, periodic solutions, as well as chaotic attractors, relevant to the asymptotic behaviors of the system.

Definition 4 *A* local attractor *is a compact set, invariant under f, which attracts its neighboring trajectories (see e.g. [14][15]).*

A global attractor is hence considered as being composed of the set of all *local attractors*, where each local attractor only attracts trajectories from a subset of initial conditions, specified by its basin of attraction. Therefore, for a fixed parameter p, different local attractors may be obtained depending on the choice of the initial condition $\mathbf{x}_0$, in contrast to the uniqueness of the case of a single global attractor.

For example, if one considers the Lorenz system with $p = 2.5$, there are three local attractors: the origin (saddle) and two symmetrical fixed points (sinks) $X_{1,2}(\pm 2, \mp 2, 1.5)$. In some cases, a unique local attractor may also be the global one. For example, when $p = 28$, there exists only a single local attractor, which is a global attractor too (known as the Lorenz strange attractor).

Definition 5 *The* ω-limit set *of a trajectory through $x \in \mathbb{R}^n$ is given as $\omega(x) = \cap_{s \geq 0} \cup_{t \geq s} \Phi(t, x)$.*

In a simplified version, the *branched manifold* defines the topological organization of all the unstable periodic trajectories which it supports [2][3][10][11]. As an example, the Lorenz branched manifold is shown in Fig. 13.

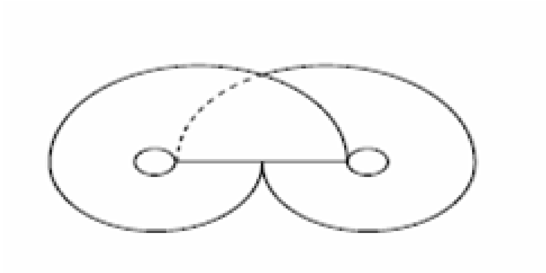

Figure 13: Sketch of the branched manifold of the Lorenz System.

References

[1] Almeida, J., Peralta-Salas, D. and Romera, M., Can two chaotic systems rise to order? *Physica D*, 200, 124–132, 2005.

[2] Birman, J. and Williams, R., Knotted periodic orbits in dynamical systems I: Lorenz's equations, *Topology* 22, 47–82, 1983.

[3] Birman, J. and Williams, R., Knotted periodic orbits in dynamical systems II: Knot holders for fibered knots, *Contemporary Mathematics*, 20, 1–60, 1983.

[4] Chen, G. and Ueta, T., Yet another chaotic attractor, *Int. J. Bifur. Chaos*, 9, 1465–1466, 1999.

[5] Christy J., Branched surfaces and attractors. I: Dynamics branched surfaces, *Trans. American Mathematical Society*, 336(2), 759–784, 1993.

[6] Danca, M.-F., A multistep algorithm for ODEs, *Dyanmics of Continuous, Discrete and Impulsive Systems, Series B*, 13, 803–822, 2006.

[7] Danca, M.-F. and Romera, M., Algorithm for control and anticontrol of chaos in continuous-time dynamical systems, *Dynamics of Continuous, Discrete and Impulsive Siystems, Series B*, (2006) accepted.

[8] Fiedler, B. and Rocha, C., Orbit equivalence of global attractors of semilinear parabolic differential equations, *Trans. American Mathematical Society*, 352(1), 257–284, 1999.

[9] Foias, C. and Jolly, M. S., On the numerical algebraic approximation of global attractors, Nonlinearity, 8, 295–319, 1995.

[10] Gilmore, R., *Chaos and attractors*, Encyclopedia of Mathematical Physiscs, EMP MS 93, 2006.

[11] Guckenheimer, J. and Holmes, P., *Nonlinear Oscillations, Dynamical Systems, and Bifurcations of Vectors Fields*, Springer-Verlag, New York, 1983.

[12] Hale, J. K., *Topics in Dynamic Bifurcation Theory*, CBMS 47, Amer. Math. Soc., 1981.

[13] Harmer, G. P. and Abbot, D., Parrondo's paradox, *Stat. Sci.*, 14, 206–213, 1999.

[14] Hirsch, M. and Pugh, C., Stable manifolds and hyperbolic setsProc. Symp. Pure Math. vol 14, American Mathematical Society, pp. 133–164, 1970.

[15] Hirsch W. M., Smale, S., Devaney, L. R., *Differential Equations, Dynamical Systems and An Introduction to Chaos*, 2nd Ed., Elsevier Academic Press, New York, 2004.

[16] Kapitanski L. and Rodnianski I., Shape and Morse theory of attractors, *Comm. Pure Appl. Math.* 53, 218–242, 2000.

[17] Letellier, C. and Gouesbet, G., Topological characterization of reconstructed attractors modding out symmetries, *J. Phys. II France*, 6, 1615–1638, 1996.

[18] Milnor, J., On the concept of attractor, *Commun. Math. Phys.*, 99, 177–195, 1985.

[19] Peitgen, H.-O. and Richter, P. H., *The Beauty of Fractals*, Springer-Verlag, Berlin, 1986.

[20] Romera, M., Small, M. and Danca, M.-F., Deterministic and random synthesis of discrete chaos, *Applied Mathematics and Computations*, 192, 283–297, 2007.

[21] Rössler, O. E., Chaos, hyperchaos and double-perspective, in *The Chaos Avant-guarde: Memories of the Early Days of Chaos Theory*, ed. by R. Abraham and Y. Ueda, World Scientific, Singapore, 2000.

[22] Salamon, D. A., Lectures on floer homology, *IAS/Park City Mathematics Series*, 7, 145–229, 1999.

[23] Temam, R., *Infinite Dimensional Dynamical Systems in Mechanics and Physics*, New York, Springer-Verlag (Applied Mathematical Sciences. Volume 68), 1988.

[24] Zelinca, I., Chen, G. and Celikovsky, S., Chaos synthesis by means of evolutionary algorithms, *Int. J. Bifur. Chaos*, in press, 2007.